

Development of a Monitoring System for Crack Growth in Bonded Single-Lap Joints Based on the Strain Field and Visualization by Augmented Reality

ANDREA BERNASCONI, MD KHARSHIDUZZAMAN, LUCA
FRANCESCO ANODIO, MONICA BORDEGONI, GUIDO MARIA RE,
FRANCESCO BRAGHIN, and LORENZO COMOLLI

Politecnico di Milano, Dipartimento di Meccanica, Milano, Italy

Received 18 July 2013; in final form 17 October 2013.

Address correspondence to Andrea Bernasconi, Politecnico di Milano, Dipartimento di Meccanica, Via La Masa 1, 20156 Milano, Italy. E-mail: andrea.bernasconi@polimi.it.

1. INTRODUCTION

Adhesively bonded joints are a very attractive solution of joining techniques over the conventional joining methods such as bolted or riveted joints, mainly due to its high strength-to-weight ratio. Especially in composite structures, adhesively bonded joints are used extensively. But due to susceptibility of bonded joints to environmental conditions and operational loading, as well as manufacturing defects such as lack of adhesion, the fatigue performance of adhesively bonded structures is a major concern even though adhesive joints show better fatigue performance than equivalent classical conventional fasteners [1]. Therefore, operational structural health-monitoring techniques are of utmost importance for damage tolerant service philosophy.

Backface strain (BFS) measurement is a very efficient technique in order to monitor crack initiation and propagation under both static and fatigue loading in adhesive joints. By this method, sensors are placed onto the exposed surface, *i.e.*, backface of the material to be bonded. Zhang and Shang [2] first assessed the use of the BFS technique in bonded joints. Their work with single-lap joint (SLJ) allowed for finding out that by detecting the switch in the direction of the BFS change, crack initiation can be monitored. However, the work of Crocombe et al. [3] regarding BFS technique was more elaborate and concluded that the BFS response was highly dependent on its location and the greatest change in BFS with damage occurs in the overlap zone. Therefore, the strain gauge should be placed on the overlap of the joint especially close to the zone where load transfer occurs. Shenoy et al. [4] investigated the crack initiation and propagation behavior in SLJ using BFS technique and showed that fatigue failure in bonded joints goes through various stages starting from an initiation period, then a slow crack growth period followed by a faster growth period before a rapid quasi-static type fracture.

In this paper, an array of strain gauge sensors is used instead of one single sensor, in order to overcome the aforementioned limitations due to the use of one single sensor. Moreover, this approach allows for evaluating the possibility of using arrays of other sensor types, like Fiber Bragg Gratings (in short FBG), which can be placed on a single optical fiber, thus simplifying the manufacturing of sensor arrays and reducing considerably the amount of wiring. FBG sensor is a very efficient tool for measuring strains in particular environments due to some great advantages such as immunity from electromagnetic interference, capacity to measure very high strain with high resolution. They match quite well with the composite materials applications, have long-term stability, and can be used at elevated temperature. The working principle of a FBG sensor is as follows [5]: the Bragg grating is made of a series of refraction index changes, spaced at a constant length period; when a Bragg grating is traversed by a white light, it reflects back only a light with a

nearly monochromatic spectrum centered on a specific wavelength, and transmits all the other wavelengths. The peak wavelength of the reflection spectra changes with the strain or temperature applied on the gratings. A special instrument, named “interrogator,” is used to gather data from the FBG sensors.

FBG sensors have a great potential in the field of structural health monitoring [6]. FBG sensors have been used successfully to detect the changes in the longitudinal strain distribution due to fatigue crack propagation in a doubler plate joint [7]. Bernasconi et al. [8] used an array of distributed FBG sensors on one side of composite adhesively bonded joints and monitored the fatigue crack growth. Da Silva et al. [9] focused on the development and testing of a technique used to measure strain levels inside an adhesive joint by FBG sensors in their work. Since several FBG sensors can be inserted in a single fiber, this enables to monitor easily the changes in the strain distribution due to the fatigue crack propagation in a joint.

The data coming from the sensors on a structure can be directly visualized by means of Augmented Reality (AR) systems. Augmented Reality is a technology coming from Computer Science that allows the user to see virtual contents in the real world [10]. This one is a highly potential technology that is continuously expanding since 1990s and it has been experimented in many different fields like marketing, medicine, military, and in industry as well. The contents are dynamically changed in real time in order to maintain a spatial and temporal coherence between the real environment and the virtual one. In this manner, the user can see the object and, at the same time, contextualized data from sensors directly on the object itself.

According to Furmann et al. [11], the use of AR to display data can be very effective. Actually, AR can speed up and enhance the human process visualization and comprehension of the data. Several investigations about the use of AR to visualize data have been already carried out. Malkawi et al. represent the air condition in a room due to an air diffuser through an immersive AR visualization [12]. Rauhala et al. developed a solution for mobile phones to represent information regarding to the humidity [13]. Goldsmith et al, instead, propose SensAR, a system to monitor the temperature and the noise level in a room [14]. White and Feiner, instead, use a mobile PC to represent the CO pollution in a neighborhood by means of an outdoor application [15]. However, according to the knowledge of the authors so far, there are no AR applications oriented to visualize information during fatigue testing. Besides, another contribution is given by the prediction and visualization of the crack growth on the specimen in real time.

This paper aims to provide a detailed investigation on the possibility of designing a monitoring system of fatigue crack growth in bonded SLJs using BFS measurements, first using relatively inexpensive electrical strain gauges to assess the feasibility of the monitoring system, then using FBGs for a more compact monitoring system, and then set a framework of a visualization tool

based on AR for real-time monitoring of fatigue crack growth in adhesively bonded joints.

2. INVESTIGATION PROCEDURE

2.1. Specimen

The type of specimen under investigation is an adhesively bonded SLJ. The substrates are aluminum 2024 T3 and HexPly[®] (Hexcel Corporation, Stamford, CT, USA) M49/42%/200P/AS4-3K carbon fiber reinforced polymer (woven, ply orientation 0°) bonded by epoxy structural adhesive DP 760 (3M Company, St. Paul, MN, USA). Two specimens were manufactured, one without artificial defects and one with an artificial crack which has been created in one side of one joint by inserting a Polytetrafluoroethylene (PTFE or Teflon) tape. The artificial pre-crack was then measured by optical microscope from two sides, one is side A where the crack length was found to be 5.7 mm and the other is side B where the crack length was found to be 8.0 mm, as shown in Fig. 1 (There is always uncertainty while creating an artificial crack by inserting a Teflon tape as its initial position inside the adhesive can be altered during bonding; therefore, we have different crack lengths in side A and side B in our case).

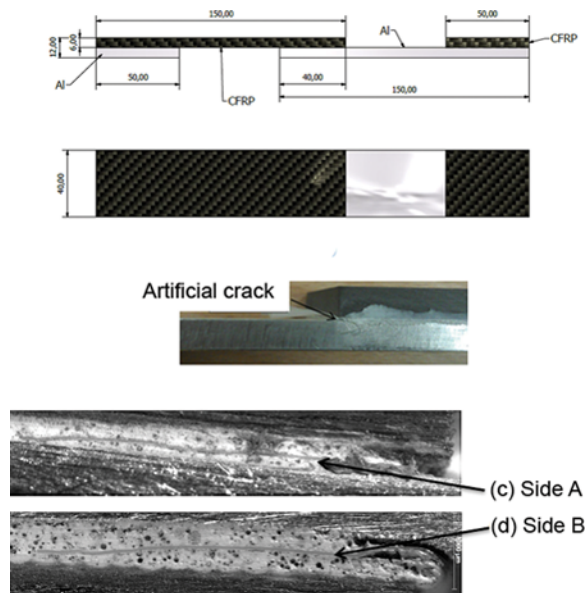


FIGURE 1 (a) Detailed dimensions (in mm) of the specimen; (b) artificial crack; (c) side A of the pre-crack, 5.7 mm long; (d) side B of the pre-crack, 8.0 mm long.

2.2. Finite Element Analysis

In order to establish the relationship between the position of the crack tip during fatigue crack propagation and the strain field to be measured by the sensors' array, a finite element (FE) model has been developed for the problem under evaluation. The FE mesh is shown in Fig. 2(a). Twenty node three-dimensional solid stress elements were used. In the case of the composite adherend, orthotropic material properties with respect to the laminae were assigned. For the adhesive, 8 node three-dimensional cohesive elements were chosen. The cohesive elements were connected to the upper and lower adherend using a kinematic constraint. The existence of the crack was modeled by modifying this length of constraint between adhesive and the aluminum adherend. Different models with different crack lengths were built and analyzed to simulate fatigue crack growth.

2.3. Correlation Between Crack Tip Position and Strain Field

A number of FE analyses were carried out by continuously varying the crack lengths and the strain values along the chosen lines shown in Fig. 2(a). From the analyses for different crack lengths, it is observed that the position of the minimum peak of the BFS values has an interesting correlation with the crack length, which is evident in Fig. 3(a), where BFS distribution along the aluminum substrate is shown starting from 5 mm prior to the overlap to 22 mm into

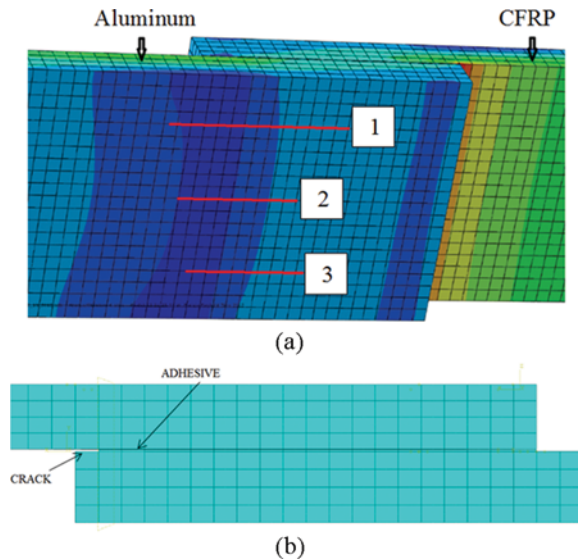
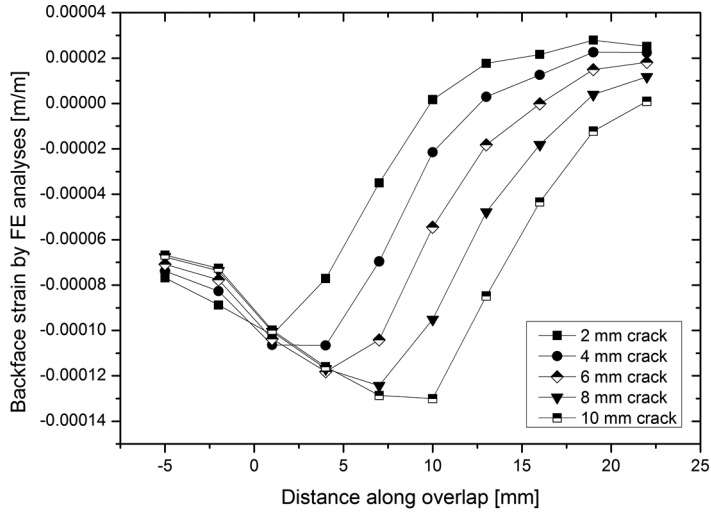
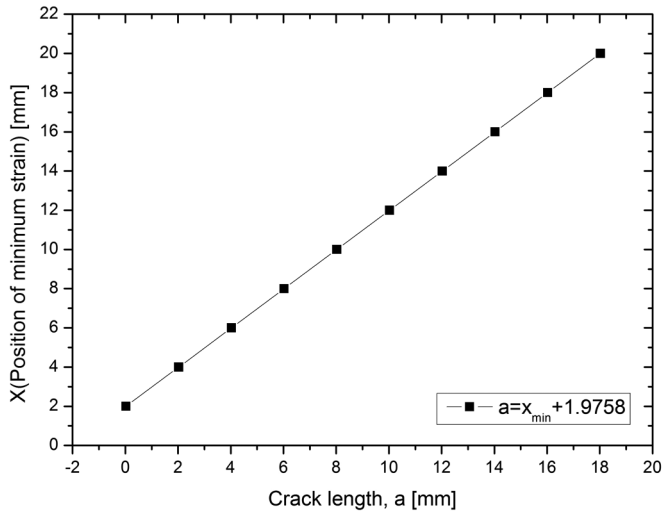


FIGURE 2 (a) Detailed FE model with three lines to be analyzed; (b) Crack modeling in the FE analysis.



(a)



(b)

FIGURE 3 (a) Results from FE analyses: backface strain for different crack lengths. (b) Correlation between the position of greatest minimum peak and the crack length.

the overlap. The BFS is plotted along the ordinate and the true distance along the overlap is on the abscissae.

It is found that the greatest minimum peak of strain profile follows the crack tip linearly with an offset of 1.98 mm. Hence the length of the crack, a , has a linear correspondence with $X_{\min \text{ strain}}$, the position of the minimum BFS, expresses by

$$a = (X_{\min \text{ strain}}) + 1.98 \text{ mm.} \quad (1)$$

2.4. Location and Application of Strain Gauges

From the FE analyses, it is observed that the greatest minimum peak of BFS curve follows the crack tip. As one of our specimens has already an artificial crack in one side of the lap joint, in order to measure the strain field with sufficient accuracy, 10 strain gauges from HBM (Hottinger Baldwin Messtechnik GmbH, Darmstadt, Germany), series 1-LY13-0.6/120 were bonded. Ten is the maximum number of gauges which can be bonded on the surface, taking into account the size and the requirements for installation. To capture the minimum peak of the BFS strain curve, we applied these 10 strain gauges in three arrays onto the backface of the aluminum substrate in that side of the joint where the pre-crack exists. It is likely that during fatigue loading, crack would start propagating from this side due to the presence of this artificial crack. The detailed configuration of the strain gauges installment is shown in Fig. 4.

For continuous monitoring of the crack propagation in the joint on the basis of the 10 strain values recorded by the strain gauges, a function has been developed in Matlab (Mathworks, Natick, MA, USA) environment based on the correlation found by FE analyses which is mentioned in Eq. (1). This Matlab function was then being used to monitor crack position during the experiment by taking the BFS values measured by the strain gauges attached to the aluminum substrate as inputs. The function scans for the minimum

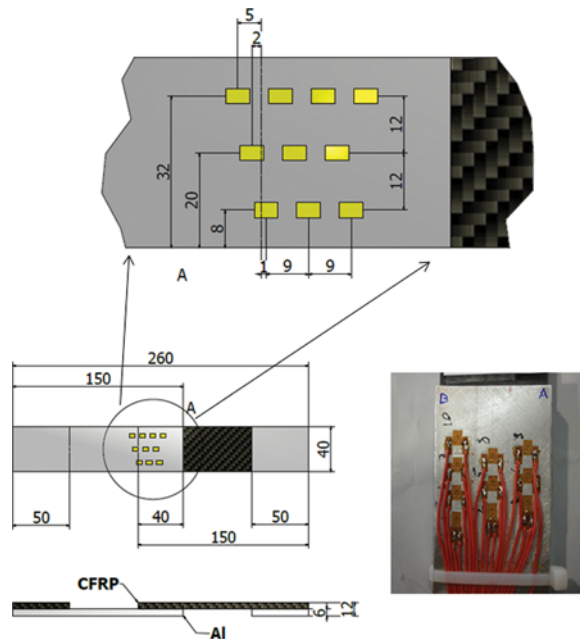


FIGURE 4 True positions of strain gauges on the specimen in accordance with the analyzed lines in FE analyses (all values are in millimeters): (a) schematic drawing and (b) installed strain gauges on the specimen.

strain value among all the strain values. Then it identifies the corresponding position of that minimum peak of BFS value on the aluminum substrate. After that, it takes into account two more strain values adjacent to the minimum peak strain value and their corresponding positions on the aluminum adherend, one just before and another just after the lowest minimum value and apply spline interpolation to accurately evaluate the position of the negative peak strain value, *i.e.*, $X_{\min\text{strain}}$ value. Then, that value is fed to Eq. (1) to identify the crack position.

2.5. Augmented Reality Framework for Real-Time Visualization

The AR framework used in this work is composed by three main modules, which have to work together in order to provide an augmented visualization to the user. Figure 5 shows the three modules. The first part regards data acquisition from sensors on the specimen and it is called Acquisition Module. These data are continuously stored in a main PC and they are used to feed the second module, called Analysis Module. Analysis Module uses the acquired data to detect the crack position according to Eq. (1). The module works in real time and it does not need any synchronization with the Acquisition Module. The Analysis Module can actually work by a pre-defined update frequency or by asynchronous user command. The data regarding sensors and crack position are then distributed by a server on the main PC to all of the devices connected. The communication is provided by a wireless network.

The third module is the AR interface. This one gets the data from the main PC and uses them to represent virtual objects on the specimen. The augmented visualization is possible by a camera and a display. The camera captures the environment, in which the specimen is placed, while the display shows the virtual contents superimposed on the camera frame. Figure 6 represents more into detail the workflow of the AR interface.

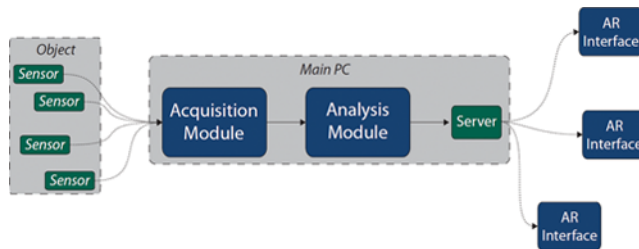


FIGURE 5 The Augmented Reality (AR) system framework. The three main modules are in blue. Data from some sensors placed on the object are acquired by the Acquisition Module and then analyzed by the Analysis Module in order to estimate the crack length. All the data are then taken by the server and distributed to all the AR interfaces connected.

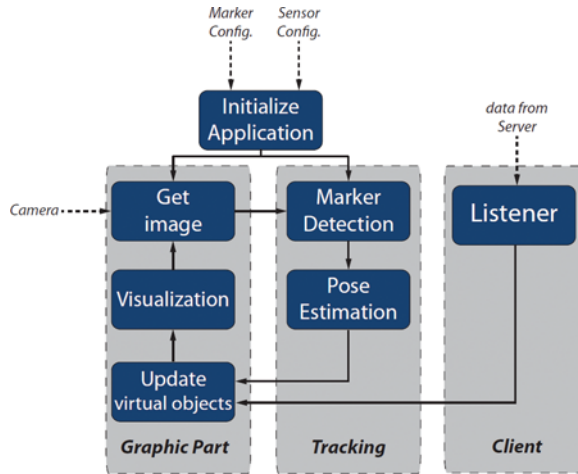


FIGURE 6 Architecture of the AR interface.

Once the camera has grabbed a new image, the tracking algorithm recognizes the markers in the scene. Then, it estimates the relative position between the camera and the marker through the coordinates of the marker vertices in the image [16]. The tracking data are then used to represent the virtual objects, as they were located on the specimen, with a proper position, orientation, and perspective. The virtual objects involved are arrows, text, and other graphics contents that can ease the data understanding to the user. A configuration file with the location of the sensors on the specimen is used to indicate to the AR interface where the virtual objects should be placed. Finally, data from the server are used to change the appearance of the virtual objects, like the textual representation of the data acquired from sensors or the crack length.

3. EXPERIMENTAL ANALYSIS AND RESULTS

3.1. Using Electrical Resistance Strain Gauges

We acquired the data from the strain gauges through two HBM (Hottinger Baldwin Messtechnik GmbH, Darmstadt, Germany) Spider 8 control units and by the software HBM Catman (Hottinger Baldwin Messtechnik GmbH, Darmstadt, Germany). The machine that applied the loads is a servo-hydraulic system MTS LandmarkTM (MTS, Eden Prairie, MN, USA) with a capacity of 100 kN. At first, we applied 2-kN static loading to the specimen in order to test the crack detection technique based on minimum negative BFS. We applied the static loading to two specimens having the same geometry and strain gauges configurations, one specimen with a pre-crack which is shown in Fig. 1 and the other one without any pre-crack. The acquired results from the static

experiments are shown in comparison with the FE analysis in Figs 7 and 8. We can see that the position of the negative peak, determined by the experiment, which is vital for crack monitoring, matched the value obtained from FE analysis. The magnitude of the BFS value in the negative peak seems to be a bit higher than the FE calculated values; this may be due to a higher bending effect in practical cases.

Then we carried out a fatigue test with the pre-cracked specimen. The machine applied a fatigue loading with a load ratio of 0.1. The maximum load at the beginning of the test was 4 kN and then it was gradually increased up to 6.8 kN with a frequency of 4 Hz. The acquisition module took the values from the sensors with a frequency of 100 Hz, collected data from the sensors, and fed to the Analysis Module every half second. In our framework, we used the Matlab function which determines crack position in the Analysis Module of the AR system. The Analysis Module takes the data acquired and it estimates the position of the crack in the specimen. In Fig. 9, the visualization through AR system at the initial stage of the experiment is shown where the BFS graph is superimposed onto the specimen and the red stripe shown refers to the crack.

From Fig. 9(a), it is clear that the initial condition of the crack length recorded by the visualization AR tool coupled with the Matlab function is in accordance with the pre-crack length measured by the optical microscope earlier. After 150 000 cycles, we recorded a crack length of 19.8 mm by means of the AR visualization tool which is shown in Fig. 9(b). In order to validate the crack length obtained by the system, we measured the crack length by an optical microscope. The value from the measurement is shown in Fig. 10 with 18.2 mm for side A and 14.3 mm for side B, probably indicating an inclined crack front.

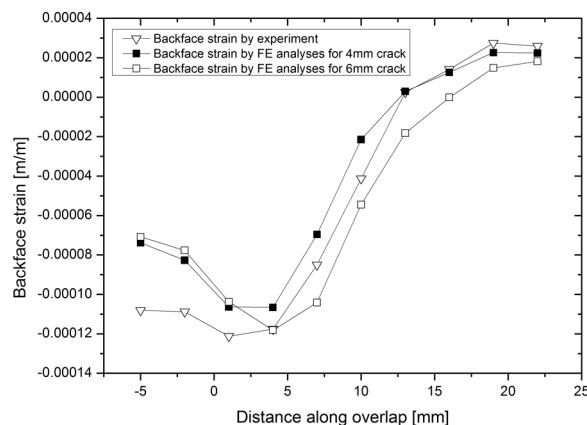


FIGURE 7 Experimental and finite element analyses for the pre-cracked specimen under a 2-kN static load.

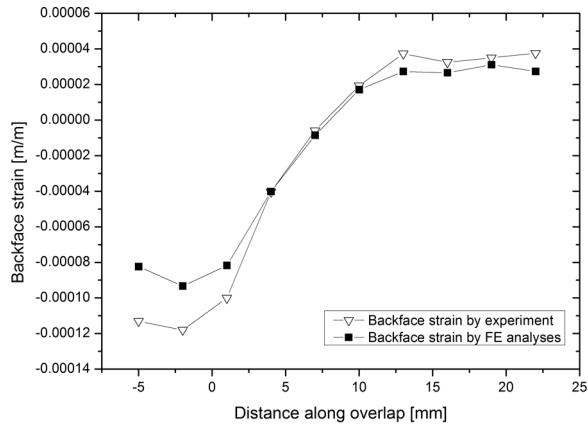


FIGURE 8 Experimental and finite element analyses for the specimen without crack under a 2-kN static load.

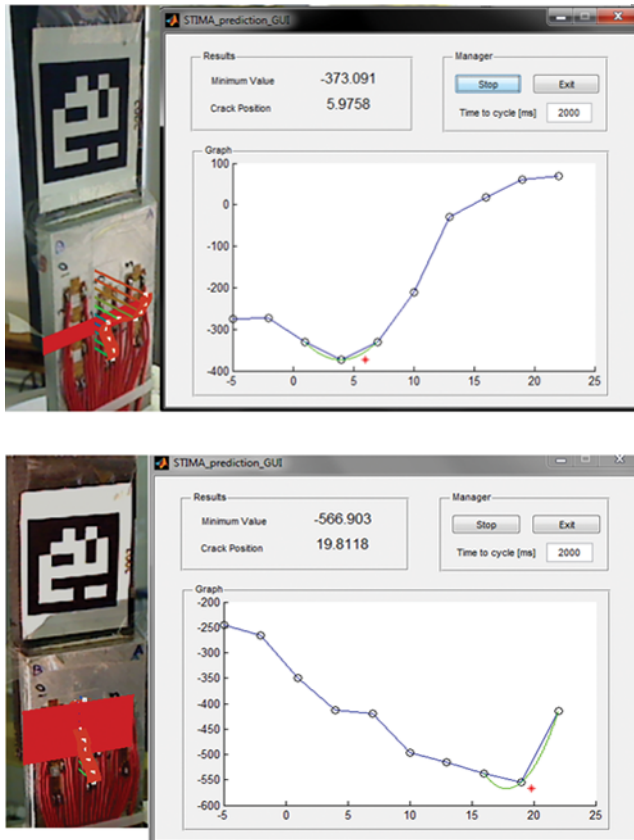


FIGURE 9 BFS graph on top of the specimen and detection and visualization of the pre-crack: (a) initial condition, (b) final condition (red stripe indicates the crack).

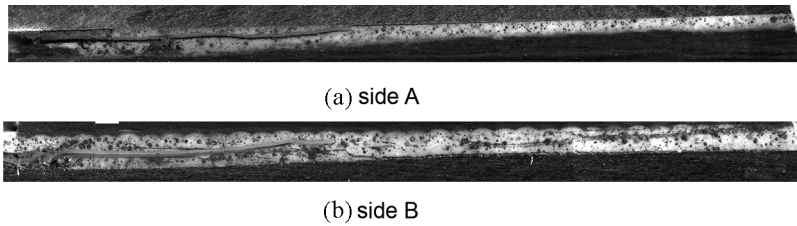


FIGURE 10 Measurement of crack by optical microscope:– (a) side A, measured crack length is 18.2 mm; (b) side B, measured crack length is 14.3 mm.

By means of this optical measurement, we found a relatively good accordance with the value we obtained by the BFS technique.

3.2. Using Optical Strain Gauges (FBG Sensors)

In the next step of the investigation, the array of strain gauges was replaced by an array of FBG sensors installed on other specimens having the same dimensions as the previous one. Also in this case, an artificial crack of 10 mm was inserted in one specimen. In this second pre-cracked specimen, care was exercised to keep the PTFE tape in position, by making it wider

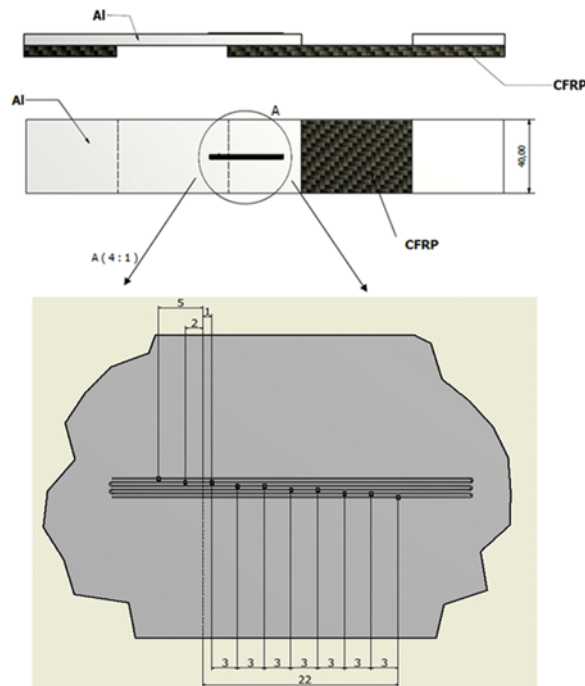


FIGURE 11 FBG sensors installation configuration (all values are in millimeters).

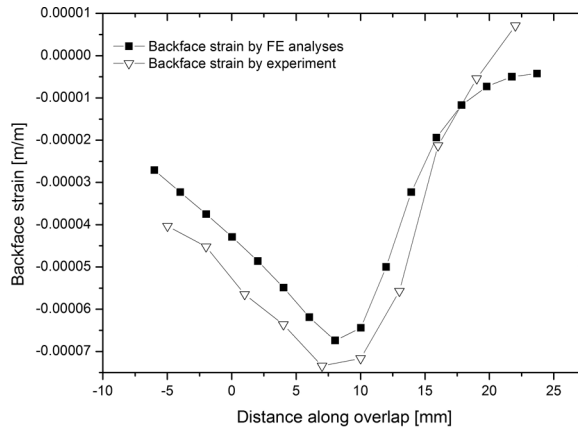


FIGURE 12 Static results for the experimental and finite element analyses for the pre-cracked specimen; strains measured by FBGs.

than the specimen. The configuration of the FBG positioning is shown in Fig. 11.

As before, at first we carried out a static test for both specimens, one without any crack and the other one with a pre-crack of length 10 mm. The results of the static analysis obtained from the experiment with the comparison of the corresponding FE analysis are shown in Figs 12 and 13.

From Figs 12 and 13, it is clear that for both cases, the position of the negative peak of the BFSs measured by FBGs is the same as the positions obtained by the FE analyses and maintains approximately a 2-mm offset from the crack tip as found in the study above. Then, we were able to visualize the experimental result for the 10-mm pre-cracked specimen in AR system coupled with the Matlab function for crack detection and monitoring

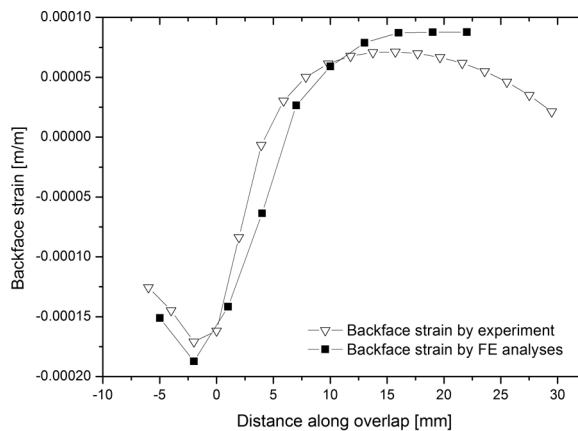


FIGURE 13 Static results for the experimental and finite element analyses for the specimen without crack; strains measured by FBGs.

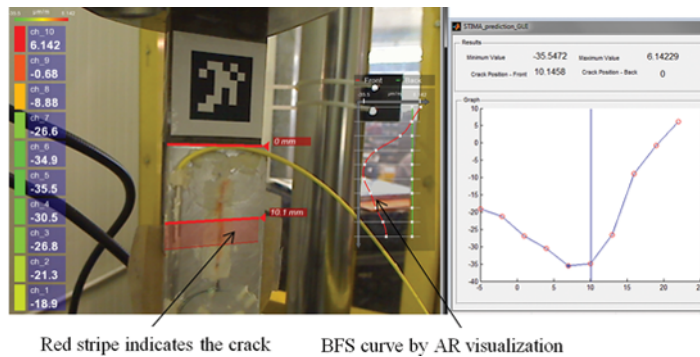


FIGURE 14 Visualization of the position and length of the crack based on negative peak detection of backface strain by FBG sensors by Augmented Reality (AR) framework (left, visualization by AR interface; right, position of the minimum BFS detection by Matlab function in the Analysis Module as seen by the vertical blue line).

(Fig. 14). It appears that by AR it is possible to display different types of information, like values of the strain recorded by the sensors, a graph of the variation of the strain values along the specimen's axis, and the size of the crack (in this case the artificial one).

Based on these preliminary results, it is possible to infer that the same procedure which was set up using strain gauges can be implemented using FBGs. It is then possible to implement the same fatigue crack monitoring and visualization technique, which, in the case of FBGs, present the advantage of a drastic reduction of the size and the number of wires which are necessary to use.

4. CONCLUSIONS

A method for structural health-monitoring system of metal-composite adhesively bonded joints in composite structures was developed, based on the detection of BFS peak detection and visualization by AR framework. By means of this methodology, it was possible to detect and monitor the crack propagation in real time in the bonded joint during a fatigue test. In this work, strain gauges were used for acquiring backface strain and to monitor crack propagation in fatigue loading. A similar framework was also adopted by replacing the electrical resistance strain gauges with optical strain gauges such as FBG sensors and the tests confirmed the feasibility of the system also with this kind of sensors.

FUNDING

This work was funded by Regione Lombardia in the framework of the project "STIMA—Strutture Ibride per Meccanica ed Aerospazio"—Bando Accordi Istituzionali—ID_Progetto: 14567

REFERENCES

- [1] Ashcroft, I. A., Crocombe, A. D., Modelling Fatigue in Adhesively Bonded Joints. In *Modeling of Adhesively Bonded Joints* L. F. M. da Silva, and A. Ochsner, (Eds.) (Springer-Verlag, Berlin, 2008)
- [2] Zhang, Z. and Shang, J. K. *J. Adhesion* **49**, 23–36 (1995).
- [3] Crocombe, A. D., Ong, C. Y., Chan, C. M., Abdel Wahab, M. M., and Ashcroft, I. A., *J. Adhes.* **78**, 745–778 (2002).
- [4] Shenoy, V., Ashcroft, I. A., Critchlow, G. W., Crocombe, A. D., and Abdel Wahab, M. M., *Int. J. Adhes. Adhes.* **29**, 361–371 (2009).
- [5] Othonos, A., *Rev. Sci. Instrum.* **68**, 4309–4341 (1997).
- [6] Udd, E., *Proceedings of IEEE*, **84**, No. 1 (1996).
- [7] Munoz, R. A. S. and Anido R. A. L., *Compos. Struct.* **89**, 224–234 (2009).
- [8] Bernasconi, A., Carboni, M., and Comolli, L., *Procedia Eng.* **10**, 207–212 (2011).
- [9] da Silva, L. F. M., Moreira, P. M. G. P., and Loureiro, A. L. D., *J. Adhes. Sci. Technol.* doi:10.1080/01694243.2012.698120 (2012).
- [10] Milgram, P., Takemura, H., Utsumi, A., and Kishino, F., Augmented Reality: A Class of Displays on the Reality-Virtuality Continuum. *Proceedings of Telemanipulator and Telepresence Technologies (Boston, MA, USA, 31 October–1 November 1994)*.
- [11] Fuhrmann, A., Loffelmann, H., and Schmalstieg, D., Collaborative Augmented Reality: Exploring Dynamical Systems. *Proceedings of Visualization '97 (Phoenix, AZ, USA, 24–24 October, 1997)*.
- [12] Malkawi, A. M. and Srinivasan, R. S., *Autom. Constr.* **14**, 71–84 (2005).
- [13] Rauhala, M., Gunnarsson, A.-S., and Henrysson, A., A Novel Interface To Sensor Networks Using Handheld Augmented Reality. *Proceedings of the 8th Conference on Human-Computer Interaction with Mobile Devices and Services (Espoo, Finland, 12–15 September, 2006)*.
- [14] Goldsmith, D., Liarokapis, F., Malone, G., and Kemp, J., Augmented Reality Environmental Monitoring Using Wireless Sensor Networks. *12th International Conference Information Visualisation* (London, UK, 9–11 July, 2008).
- [15] White, S. and Feiner, S., SiteLens : Situated Visualization Techniques for Urban Site Visits. *Proceedings of the 27th International Conference on Human Factors in Computing Systems (Boston, MA, USA, 4–9 April, 2009)*.
- [16] Kato, H. and Billinghurst, M., Marker Tracking and HMD Calibration for a Video-Based Augmented Reality Conferencing System, *Proceedings of IEEE and ACM International Workshop on Augmented Reality (San Francisco, California, USA, 20–21 October, 1999)*